

Historical trends in Crop Water demand over Semi-Arid region of Syria

Rajab Homs

Universiti Teknologi Malaysia

Shamsuddin Shahid

Universiti Teknologi Malaysia

Zafar Iqbal (✉ zafar.thalvi@gmail.com)

Universiti Teknologi Malaysia

Atif Muhammad Ali

Hohai University

Ghaith Falah Ziarh

Universiti Teknologi Malaysia

Research Article

Keywords: Climate change, Crop Water Stress, general circulation model (GCM), Syria

Posted Date: April 13th, 2021

DOI: <https://doi.org/10.21203/rs.3.rs-394301/v1>

License:  This work is licensed under a Creative Commons Attribution 4.0 International License.

[Read Full License](#)

Version of Record: A version of this preprint was published at Theoretical and Applied Climatology on August 21st, 2021. See the published version at <https://doi.org/10.1007/s00704-021-03751-5>.

Historical trends in Crop Water demand over Semi-Arid region of Syria

Rajab Homs¹., Shamsuddin Shahid¹, Zafar Iqbal^{1*}, Atif Muhammad Ali² and Ghaith Falah Ziarh¹

¹School of Civil Engineering, Faculty of Engineering Universiti Teknologi Malaysia (UTM),
81310 Johor Bahru

²College of Hydrology and Water Resources, Hohai University, Nanjing, China

Corresponding Author: Zafar Iqbal
Email zafar.thalvi@gmail.com

Historical trends in Crop Water demand over Semi-Arid region of Syria

Abstract

Climate change has caused a shift in aridity, particularly in the dry regions of the world which may subsequently affect several sectors predominantly the agricultural and water resources. This research examined the climate change effects on crop water demand (CWD) in Syria over the period 1951-2010. Given the lack of observed data, this analysis relied on (GPCC) precipitation and (CRU) temperature data from 1951 to 2010. Potential Evapotranspiration (PET) at each grid was calculated using Penman-Monteith method and FAO-56 model was used to calculate the crop water demand (CWD). The analysis revealed that CWD in Syria increased from 1981 to 2010 when compared to 1951-1980. The increase in CWD has been found for all the crops except wheat, whereas the maximum changes are found during April, and May. The differences in CWD for Barley between the two periods were found to be in the range of -20 to 40 mm. A decrease in CWD observed in the south of the country. However, a rise in 0 to 20 mm range was also discovered in the north. The CWD for wheat was found to decline in most parts of the country. However, it was found to increase in the north. The increase in CWD for barley and wheat has increased agricultural water stress in the region. Several agriculture planning needs to be developed in accordance with the expected future climate changes in order to maintain the agricultural production in the region.

Keywords: Climate change, Crop Water Stress, general circulation model (GCM), Syria

Introduction

Rapid environment changes due to unsustainable human activities have created numerous challenges across the world. The rise in temperature due to anthropogenic activities causing the increase in Greenhouse gases (GHG) eventually alters the rainfall distribution and intensity (Scherer et al., 2014, Wang et al., 2014, Iqbal et al., 2019, Swain et al., 2016). Changes in precipitation rate, frequency, and distribution are causing a rise in hydrological hazards around the world. (Mayowa et al., 2015, Noor et al., 2019). Because of their fragile ecosystems, Arid and semi-arid temperature zones are more complicated even to minor shifts in climatic conditions. (Mehrotra et al., 1995, Samadi et al., 2012). Arid areas are often characterized by extremely dynamic hydrological processes that often demonstrate unusual behavior, for example flash flooding caused by substantial precipitation and water stress induced by a lengthy dry spell (Buytaert et al., 2012). However, water stress due to less rainfall and higher temperature are found to be more frequent in arid regions compared to other hydrological disasters (Miyan, 2015). It has been projected that water stress will become more frequent and severe in the arid region in the future creating increase in crop water demand (Nam et al., 2015, Boretti et al., 2019).

Global warming-induced surface temperatures have modified evapotranspiration, air moisture retention potential and, as a result, the seasonal and spatial distribution of rainfall (Wang et al., 2016b). The Intergovernmental Panel on Climate Change (IPCC) estimates that increased in water scarcity has been recorded in many regions as a result of rising temperatures and dry periods, especially in Asian countries. Reduction in crop production due to water stress has also been stated in a number of studies (Bates et al., 2008). The situation may be adverse in west of Asia and Middle East region due to higher increase in temperature (Houmsi et al., 2019). Studies showed a rise in temperature at a much higher rate in Middle East compared to many other regions (Salman et al., 2018). Unlike many other regions, precipitation in Middle Eastern region has been projected to decrease when the temperature rises (Lelieveld et al., 2012). These changes can lead to the impacts which are linked to shifting in aridity and the specific requirement of water level by different crops (Acreman et al., 2009, Wheeler et al., 2004, Houmsi et al., 2019). Because of climate change, water balance changes that are responsive in relation to topographical, geographical, and climatic controls can disrupt soil heterogeneity and agricultural operation (Houmsi et al., 2019). If appropriate steps are not taken, this may have a detrimental effect on the region's livelihood and economic activities (Ahmed et al., 2019, Khan et al., 2018).

Aridity has been found increasing in major parts of the world particularly in Middle Eastern countries. Houmsi et al. (2019) evaluated the aridity expansion in Syria from 1981-2010. The study reported that the decrease in rainfall has instigated the changes in aridity. In the period 1951-1980, a total of 6.21 percent of semi-arid land has been turned to arid. El Kenawy et al. (2016) applied Pinna Index and De Martonne index to analyze the changes in aridity of Middle East and Northern African region, he found that the aridity is increasing over the humid regions more rapidly. Asadi Zarch et al. (2017) employed aridity index established by UNESCO to assess the aridity on a global scale using GCMs. According to the results of this study, an increase in arid, semi-arid, and sub-

humid areas is expected. Whereas, hyper-arid and humid zones will be decrease all over the world. Sahour et al. (2020) reported the statistically significant increase in trend of aridity in major part of Middle East.

Agriculture is the most vulnerable field to climate change. because it relies so heavily on water resources (Zhang et al., 2012). In most of the arid regions, rural economies are highly dependent on agriculture land use in which cultivation is highly productive but restricted to the limited land area due to the unavailability of water (Nautiyal et al., 2015). Crop water demand applies to the amount of water needed to compensate for evapotranspiration losses from field crops (Liu et al., 2013b). Sun et al. (2018) the agricultural water demand in the Loess Plateau of northern Shaanxi was evaluated, under three future climate change scenarios. The findings revealed a downward trend in irrigation water demands for major crops under future climate change scenarios. The RCP8.5 (0.90%) has the highest decreasing trend in irrigation water demand, RCP4.5 (0.77 %) and RCP2.6 (0.30 %) per year. Liu et al. (2013a) investigated spring highland barley crop water demand and deficit in China's Tibet region. The study found that deficit in water required for the crop with different spatial distribution. Azad et al. (2018) studied that Climate change has an effect on wheat yield in Myandoab, Iran. According to the findings in 2055, temperature and reference evapotranspiration will rise. Temperature rises will result in a decrease in crop growing season and crop evapotranspiration. The negative effect of rising temperatures outweighs the positive effect of rising CO₂ levels and lower yields. Brouziyne et al. (2018) have used SWAT model and downscaled GCMs to investigate the effect of climate change on the water requirements of winter wheat and sunflower in northwestern Morocco.

The lack of water affects the livelihood of the vast population when it occurs in an arid region (Al-Furaiji et al., 2016). Climate-induced variations in the frequency and severity of agricultural water scarcity, can cause severe and long-lasting effects on agriculture, livelihood and natural systems if adequate adaptation plans are not implemented (Nam et al., 2015). Understanding recent and expected future developments is vital, the successful climate change adaptation plans must be implemented (Wang et al., 2016a). Therefore, in the present study a frame work for assessing the changes in crop water demand for data scares region has been developed for Syria. To our knowledge and extensive literature review, so far, no research has been done using gridded data sets to examine historical shifts in crop water demand in Syria.

Study Area

Syria is situated in the Middle East and covers an area of 185,180 km². Its latitude ranges from 32° to 38°N and its longitude ranges from 35° to 43°E. The country is bordered on the west by the Mediterranean Sea and Lebanon, on the north by Turkey, on the south by Jordan, and on the east by Iraq. The country's topography is defined in the west by a narrow coastal plain, mountains in the west, and a desert plateau in the east. (Figure 1).

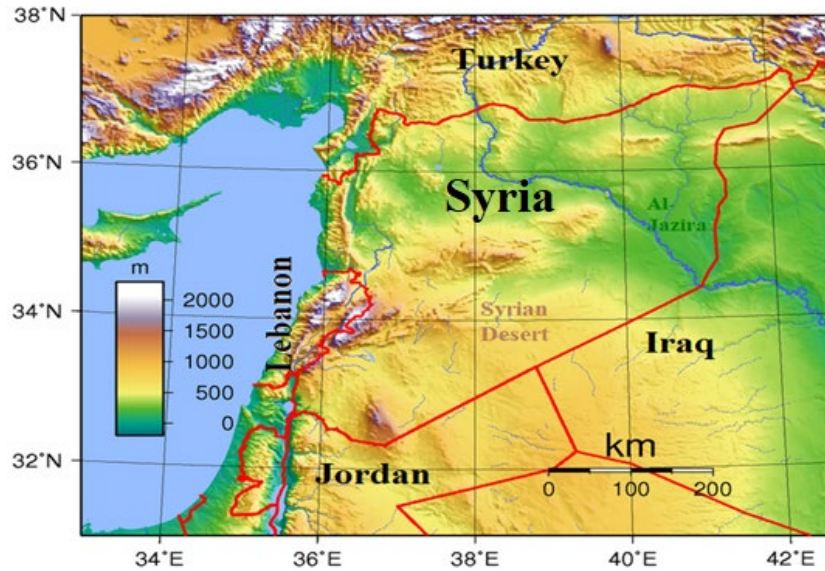


Figure 1 Location in the world and topography of Syria

The country has two distinct seasons: a warm summer (May to October) and a cool, rainy winter (November to April). The average daily maximum temperature varies from about 40°C in summer to 12°C in winter. The average daily minimum temperature goes down to 2°C in winter. The summer minimum temperature is around 20°C. The seasonal variation of temperature in Syria is given in Figure 2.

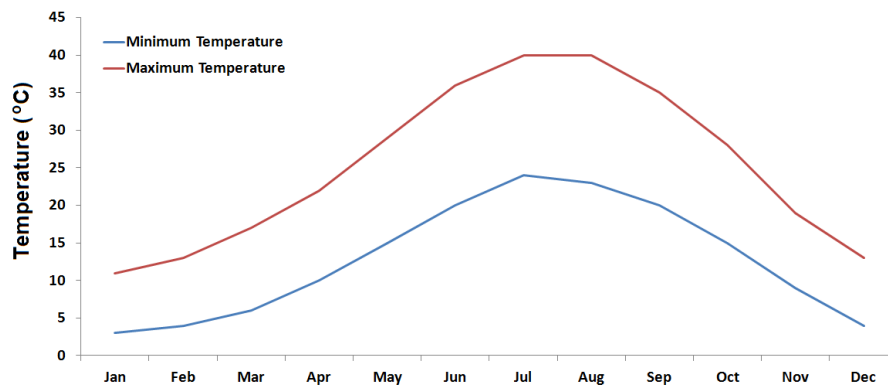


Figure 2 The seasonal variation of temperature of Syria estimated using climate research unit (CRU) temperature for the period 1951-2010.

The Mediterranean winds carries moist air. Syria receives much of the precipitation throughout the winter (November to May). The precipitation occurs in the form of snow and ice in the north. In most parts of the world, the summer months see virtually no rainfall. The country's rainfall

varies between 75 and 1000 millimeters each year. Syria's seasonal variation in precipitation is presented in Figure 3.

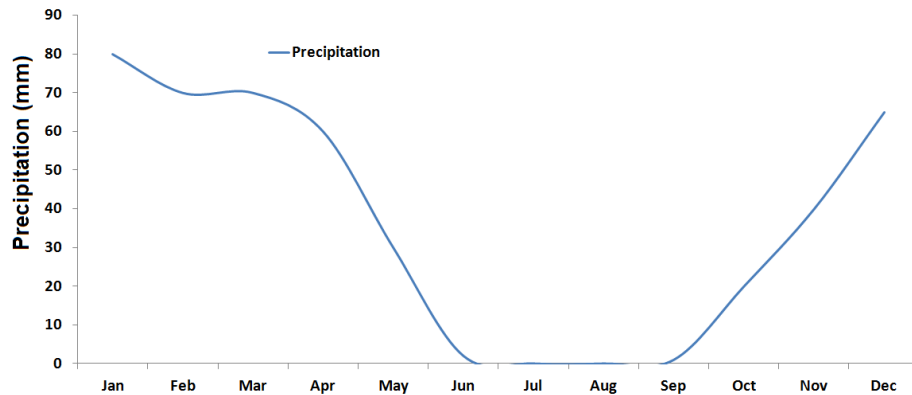


Figure 3 The seasonal variation of precipitation of Syria estimated using global precipitation climatology centre (GPCC) precipitation for the period 1951-2010

Data

Gridded data sets

Various gridded data were used in this study, including precipitation data from the (GPCC, V.7) (Becker et al., 2013), temperature data from the (CRU) (Harris et al., 2014), in addition to Princeton University Global Meteorological Forcing Dataset (PGF) (Sheffield et al., 2006). These three products were used because it is widely used in various researches globally whereas in our previous research Houmsi et al. (2019), it was found most suitable for the Syrian region

Table 1 Details of Gridded data

Products	Source and Abbreviation	Temporal Resolution	Spatial Resolution	Geographical Coverage
GPCC (Becker <i>et al.</i> , 2013)	Global Precipitation Climatology Center, GPCC v.7 (http://www.esrl.noaa.gov/psd/data/gridded/data.gpcc.html)	Monthly (1901–2010)	0.5°×0.5°	Global, Land only

CRU (Harris <i>et al.</i> , 2014)	The University of East Anglia Climatic Research Unit, CRU TS 3.22. https://crudata.uea.ac.uk/cru/data	Monthly (1901–2013)	0.5 ⁰ ×0.5 ⁰	Global, Land only
Princeton (Sheffield <i>et al.</i> , 2006)	Global Meteorological Forcing Dataset for land surface modeling http://hydrology.princeton.edu/data.pgf.php	Daily (1948–2010)	0.25 ⁰ ×0.25 ⁰	Global, Land only

Syria has two major crop growing seasons, Winter and Summer. About 73% of the total agriculture land of Syria is cultivated during winter (Houmsi *et al.*, 2019). The major crops of Syria include wheat, barley, cotton, tobacco, and grapes. Among that wheat and barley are growing during winter and cotton, tobacco and grapes are grown during summer. The calendar for Syria's chosen crops is shown in Figure 4

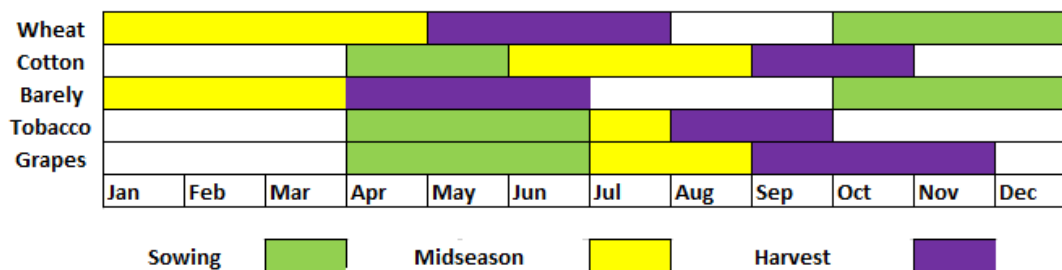


Figure 4 Calendar for selected main crops of Syria (FAO, 2017)

Cropping seasons in Syria differ only by a few days between irrigated and rain fed areas. The rainfall is often correlated with the time of rainfall in the rain-fed region. . As a result, the winter crop season is more regular in irrigated areas than in rain-fed areas, with increased quantity and quality at a higher rate. The periods used for the estimation of CWD for different crops are given in Table 2.

Table 2 The periods used for the estimation of CWD for different crop growing (FAO, 2017)

Crops	Period(day)	Season (months)
Wheat	240	October to April
Cotton	195	April to July
Barley	195	October to June
Tobacco	150	April to July
Grapes	210	April to September

3.0 Methodology

In this study the difference in Crop water demand for various crops (Barley, Cotton, Tobacco, Grapes and Wheat) were analyzed for the period of 1951-1980 and 1981-2010 using gridded historical data. The Procedure adopted in this study is as under

1. The Potential Evapotranspiration was calculated using Penman-Monteith method at each grid for the period of 1951-1980 and 1981-2010 using gridded data.
2. The crop water demand was calculated for each grid using FAO-56 model
4. The spatial distribution of changes in CWD for Syria for various crops are calculated and plotted using ArcGis

The details description of the methods used are stated below

3.1 Penman-Monteith Potential Evapotranspiration Calculation Method

The system used to estimate PET has a major effect on the CWD value. PET can be estimated using a variety of techniques. Their accuracy varies depending on data availability, temporal scale, application, and climate condition (Berg et al., 2017). According to studies, the FAO Penman-Monteith model (Allen et al., 1998) will calculate PET with greater precision in any area of the world (Berg et al., 2017). As a result, it has been observed as a common procedure method for estimating Potential evapotranspiration all over the world (Muhammad et al., 2019). In this study, the FAO Penman-Monteith empirical method for estimating PET was used.

$$PET = \frac{\Delta R_n + 0.4244 (1 + 0.536u_2)(e_s - e_a)}{(\Delta + 0.067)(2.501 - 0.00236T)} \quad (1)$$

Where PET is measured in millimetres each day, u_2 is the wind speed at 2 meters above the surface (m/h), T is the temperature ($^{\circ}\text{C}$), e_s is the saturation vapor pressure (KPa), e_a is the real vapor pressure (KPa), $\frac{de_s}{dT}$ is the gradient of the saturation pressure curve (KPa/ $^{\circ}\text{C}$), and R_n is the earth's surface net radiation (MJ/m²/day).

The mean saturation vapor pressure (e_s) was calculated from air temperature, while the real vapor pressure (e_a) was calculated from relative humidity. Saturation vapor pressure and temperature were used to measure the slope of saturation vapor pressure.

3.2 Estimation Methods of Crops Water Demand

Precipitation (P) and potential evapotranspiration (PET) essentially define water balance (Thornthwaite, 1948, Tsakiris et al., 2005). The water balance equation was used to predict water demand for various crops (Kar et al., 2005).

The FAO-56 model (Brouziyne et al., 2018) was used to calculate irrigation water demand. The CWA for the i-th month is described as the difference between the monthly precipitation, P_i , and PET_i

$$CWA_i = P_i - PET_i \quad (2)$$

The total irrigation water requirement or crop water demand (CWD) can be calculated as:

$$W_{irr} = ET_{crop} - P_e \quad (3)$$

W_{irr} irrigation water requirements

ET crop evapotranspiration

P_e effective precipitation

The formula for calculating crop evapotranspiration is:

$$ET_{crop} = EC \times ET_{ref} \quad (4)$$

where:

The crop coefficient is denoted by EC, and the reference evapotranspiration is denoted by ETref.

The term "effective precipitation" refers to the portion of rainfall that can be used to fulfil the evapotranspiration needs of growing crops. Using the USDA equation, effective precipitation is calculated (United States Department of Agriculture 1983) as given below:

$$Pe = SF \times (0.70917P - 0.82416Pt - 0.11556) \times 100.02426 ET \quad (5)$$

Pt is the monthly average precipitation (in inch), and Pe is the mean monthly effective precipitation (in inch). The soil water storage factor is denoted by SF. And ET is the average monthly crop evapotranspiration (in inch). The soil water storage factor is described as follows:

$$SF = (0.531747 + 0.295164 D - 0.057697 D^2 + 0.003804 D^3) \text{ Error!} \quad (6)$$

No text of specified style in document..1

Where D denotes the amount of available soil water storage (in inch). Subjected on the irrigation management methods employed, in the crop root area, the term D is normally estimated to be 40% to 60% of the usable soil water capacity (United States Department of Agriculture 1970). In this scenario, D is expected to be 50% of the soil water capacity.

4.0 Results

4.1 Areal Average Trends of Meteorological Variables

The meteorological variable maps used in the Penman-Monteith system for PET estimation are shown in Figure 5. In Syria, the annual mean of daily relative humidity and wind speed varied from west coast to inland. The relative humidity difference was discovered to decline from 75% in the tropical northwest to 45% in the desert in the southeast. Wind speeds decreased from 4.3 miles per hour in the northwest to less than 2.8 miles per hour in the northeast. As it has been

discovered, solar radiation varies with latitude. The country's southeast received the most solar radiation (7.3 W/m^2).

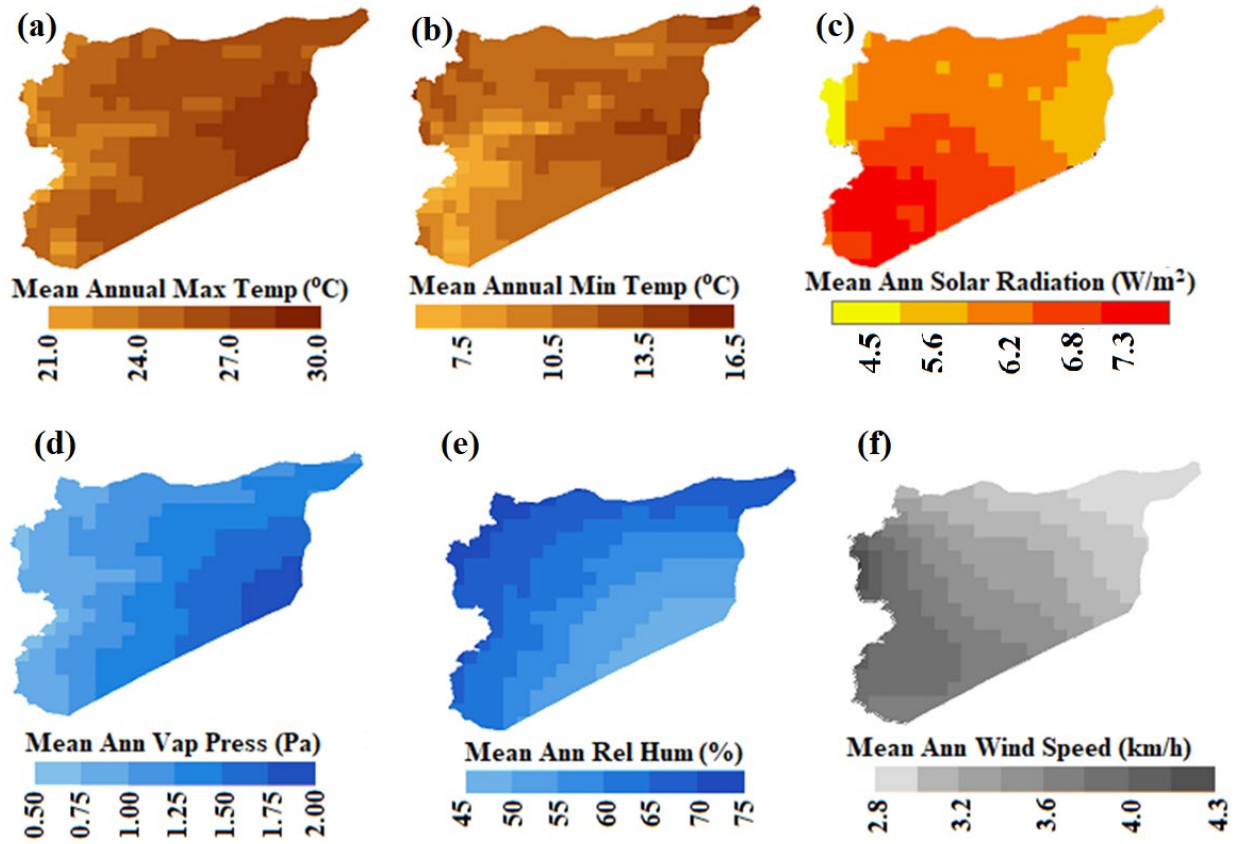


Figure 5 Annual Average of (a) Maximum Temperature (b) Minimum Temperature (c) Solar Radiation (d) Vapor Pressure (e) Relative Humidity (f) Wind Speed

Figures 6-9 represent variations over the study period, in numerous meteorological factors and aridity (1951-2010). For the period 1951-2010, the anomaly series was formed by subtracting the mean from the areal average values of meteorological variables. The anomaly series represented the shifts in aridity and other meteorological factors over time. In recent years, the mean temperature has hardly changed while the minimum temperature has risen. The PET has been observed to rise in recent years, while rainfall has declined. The overall relative humidity

throughout the country remained almost unchanged. The AI in the region was discovered to be declining because of a rise in potential evapotranspiration and a decline in precipitation.

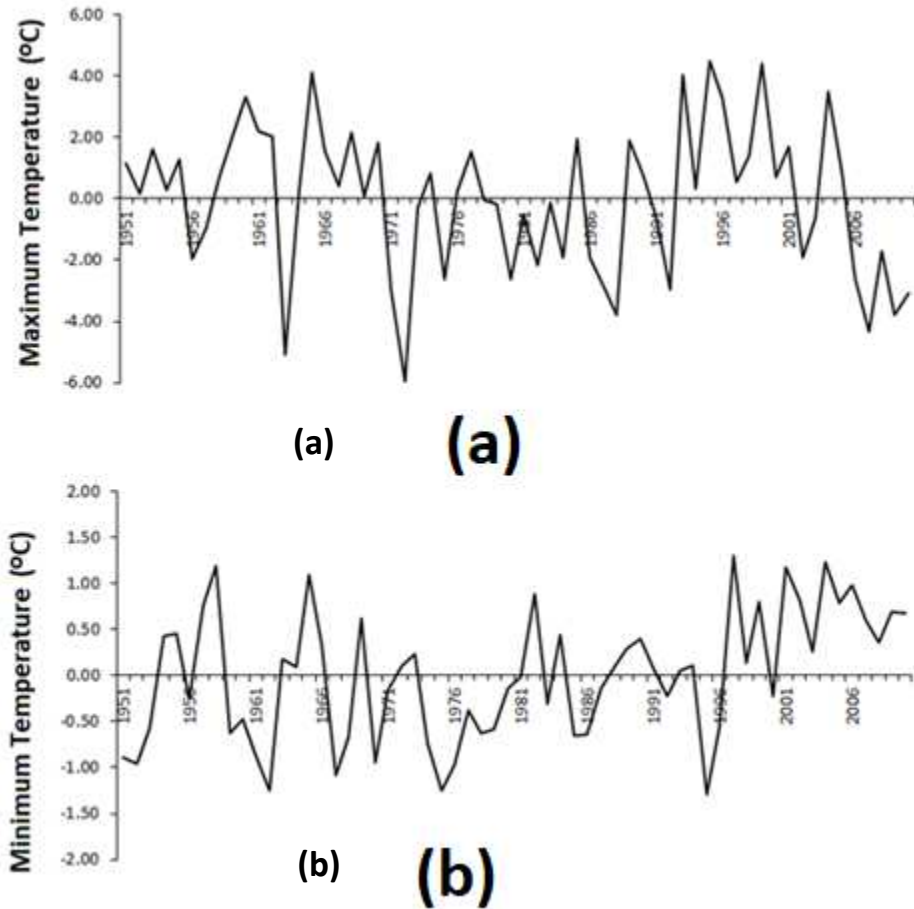


Figure 6 Anomaly in an annual average of daily (a) maximum temperature, and (b) and minimum temperature

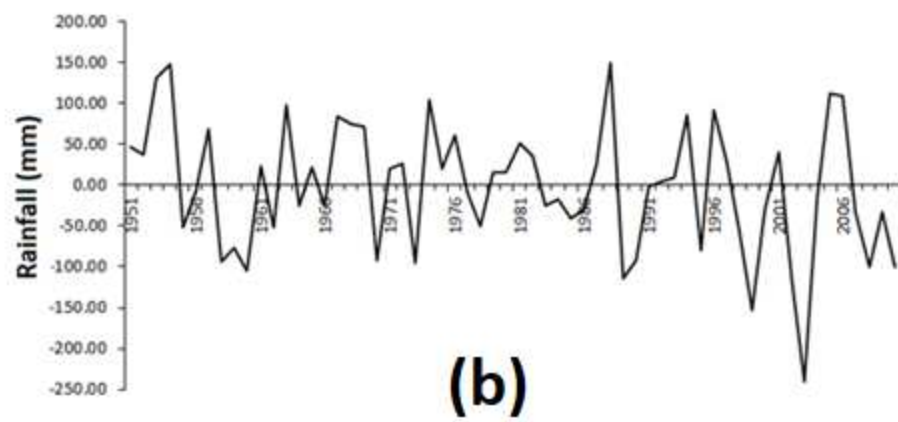
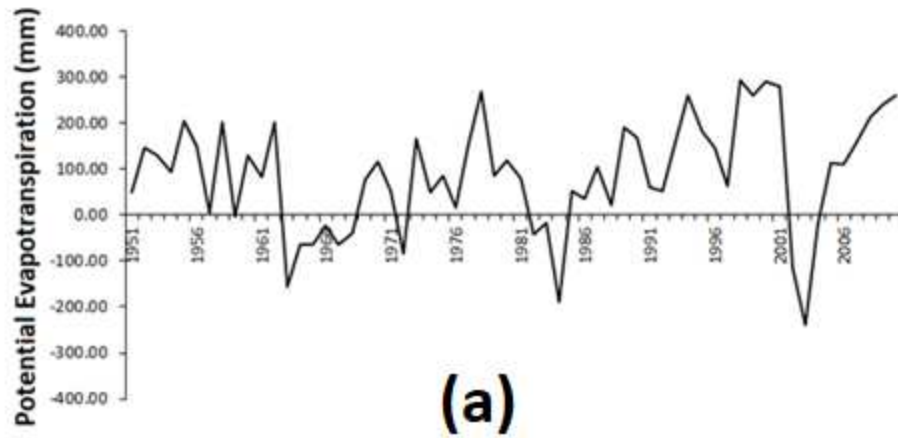


Figure 7 Anomaly in annual (a) potential evapotranspiration, and (b) rainfall

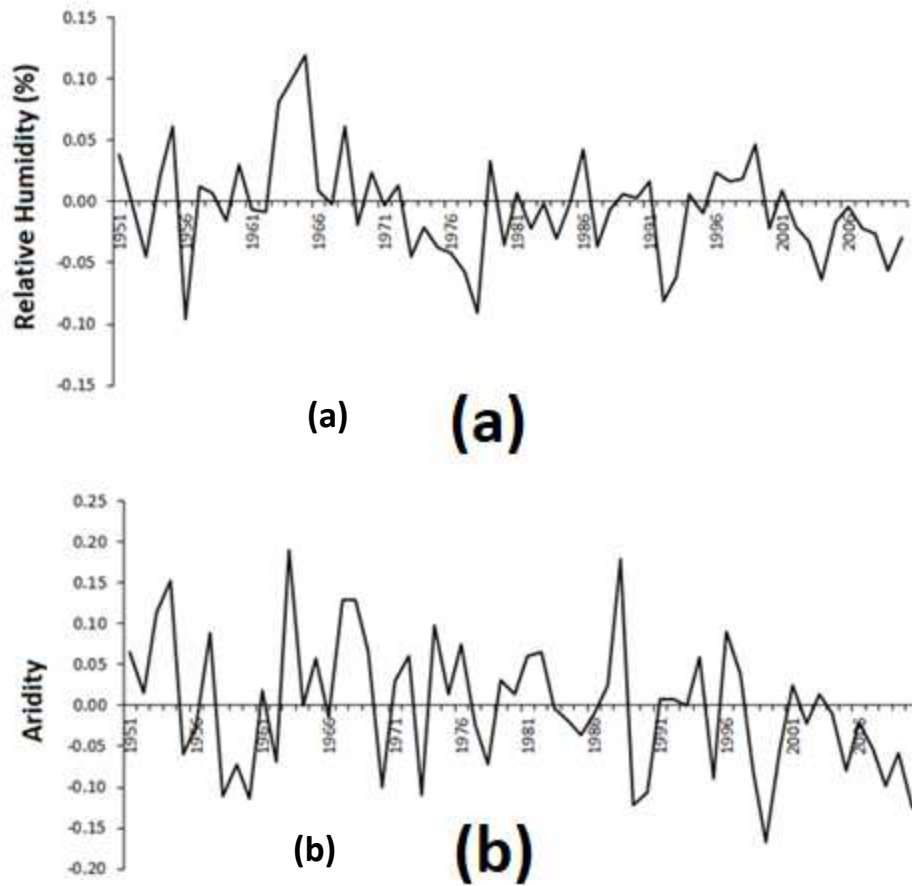


Figure 8 Anomaly in annual average (a) relative humidity, and (b) aridity

4.2 Estimation of the Spatial Distribution of Potential Evapotranspiration

The Penman-Monteith method was used to measure the PET, as shown in Figure 9. The Potential evapotranspiration rose from 1600 mm in the northwest to 2800 mm in the southeast. Because of the high PET in comparison to rainfall, the majority of the country has an arid climate.

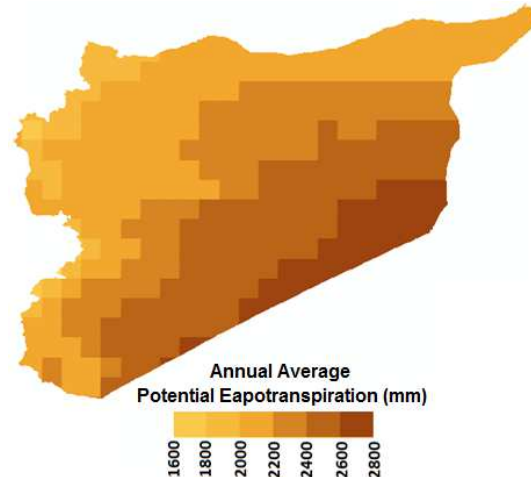


Figure 9 The Penman-Monteith method was used to calculate the spatial distribution of potential evapotranspiration (mm).

4.3 Geographical Distribution of Rainfall, Temperature, and Potential Evapotranspiration Trends

To better comprehend the reasons of changes in CWD, the spatial distribution of variations in rainfall and temperature, as well as PET, were measured and the findings were analysed and are given in Figures 10, respectively. Used Sen's slope to evaluate variations in rainfall, temperature, and PET, the significance of the changes was evaluated using MMK test with a significance level of 0.05 from 1951 to 2010. Rainfall variations were estimated to range from 4 to -32.0 mm/decade. The north and northeast experienced a significant decrease in precipitation. The declining rate was discovered to be greater than 32 millimetres/decade in the northeast, where the average annual rainfall is around 800 mm. Rainfall in the northern semi-arid zone has declined by 12 to 16 mm per decade. where average annual precipitation is 300 to 400mm. This means that precipitation is steadily falling in the country's north and northeast.

The country's temperature has been shown to increase dramatically across the board. The increase was discovered to be larger in high temperature regions and comparatively smaller in low temperature regions. The largest increases were witnessed in the east, especially in the northeast (0.28°C/decade). Furthermore, it was discovered to be steadily rising in the northwest (0.17°C/decade). Potential evapotranspiration, on the other hand, did not substantially increase at

any place except one point in the south-eastern desert. Figure 10 (c). The spatial pattern of the Potential evapotranspiration trend was discovered to adopt the temperature trend, showing that temperature influences the country's PET. Rising temperatures contributed to a rise in PET in most areas of the region, but the rises are not statistically yet. The rising temperature pattern, on the other hand, may trigger a rise in PET in the future.

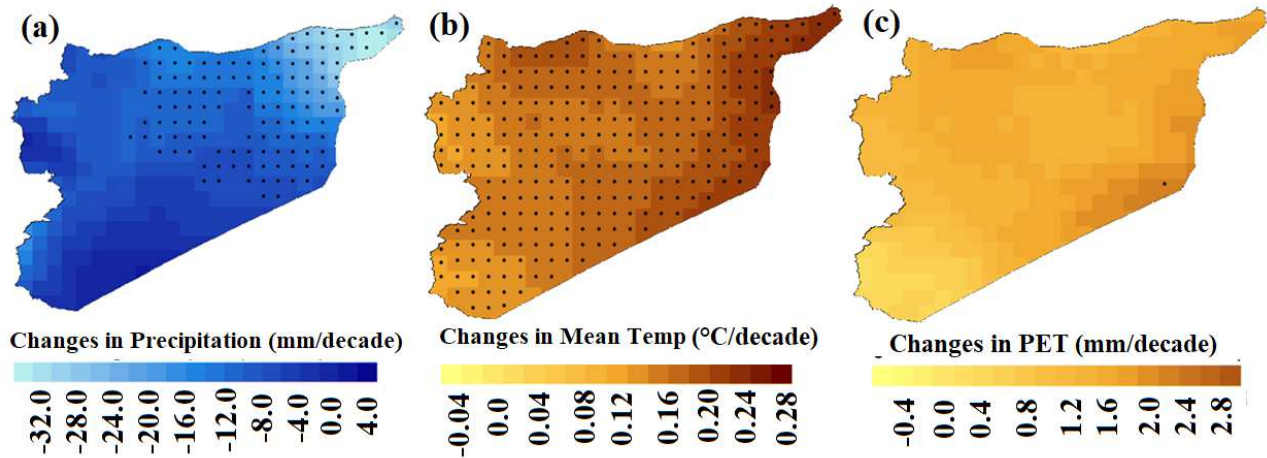


Figure 10 From 1951 to 2010, the spatial distribution of rainfall (a), temperature (b), and PET (c) . The Modified Mann Kendall trend test yielded significant trends at the 0.05 are marked as dots

4.4 Historical Changes in Irrigation Demand for Major Crops

The Wilcoxon rank test was used to evaluate shifts in CWD over two time periods: early 1951-1980 and late 1981-2010. Figure 10 illustrates the collected findings for different crops. The + and – symbols signify major increases and decreases, respectively.

Figure 11 indicates a substantial rise in CWD in the late period (1981-2010) relative to the early period (1951-1980) for all crops at 95 percent of the level of confidence. Except for wheat, all other crops were found to suffer from water scarcity in the late period while compared to the initial period. The CWD for wheat was found to decrease in April. Reduced rainfall and rising temperatures have resulted in higher CWD for most Syrian crops. Except for wheat, the greatest

rise in CWD was observed in April and May for all crops. This shows increased water tension in recent years, mostly for summer crops.

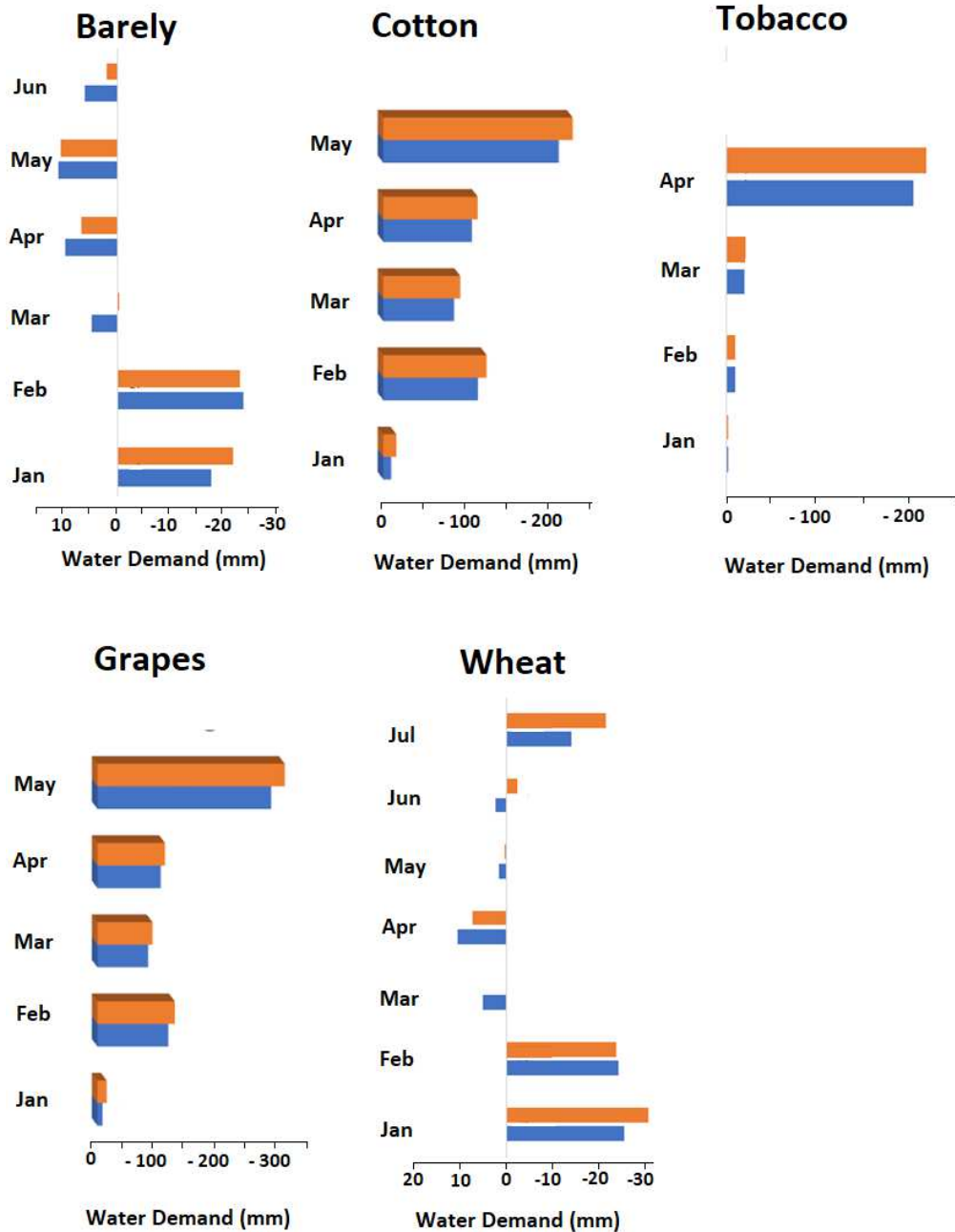


Figure 11 Changes in water demand of major crops of Iraq between 1951-1980 and 1981-2010

4.4 Spatial Distribution of Changes in CWD

Variations in CWD at various grid points in Syria between 1951 and 1980 and 1981 and 2010 are shown in Figure 12 to depicts the spatial trend in CWD transition. The map's color ramp depicts the sum of shift over two time periods.

The changes in CWD for Barley between the two periods were found in the range of -20 to 40 mm. The negative value of CWD indicates a decrease in CWD while a positive value indicates an increase. A decrease in CWD observed in the south of the country. However, a rise in the range of 0 to 20 mm was also observed in the north. . As agricultural activities of the country are mostly concentrated in the north, it can be remarked that CWD for Barley has increased in the country. In the case of cotton, grapes and tobacco, no major improvements in the CWD were noticed in any of the country's regions. Wheat CWD has been found to be decreasing in most parts of the country. However, it has been discovered to grow in the north and northeast, where it is cultivated. Overall, the findings suggest a rise in CWD for Syria's two main crops, wheat and barley. The increase in CWD for barley and wheat has increased agricultural water stress in the region.

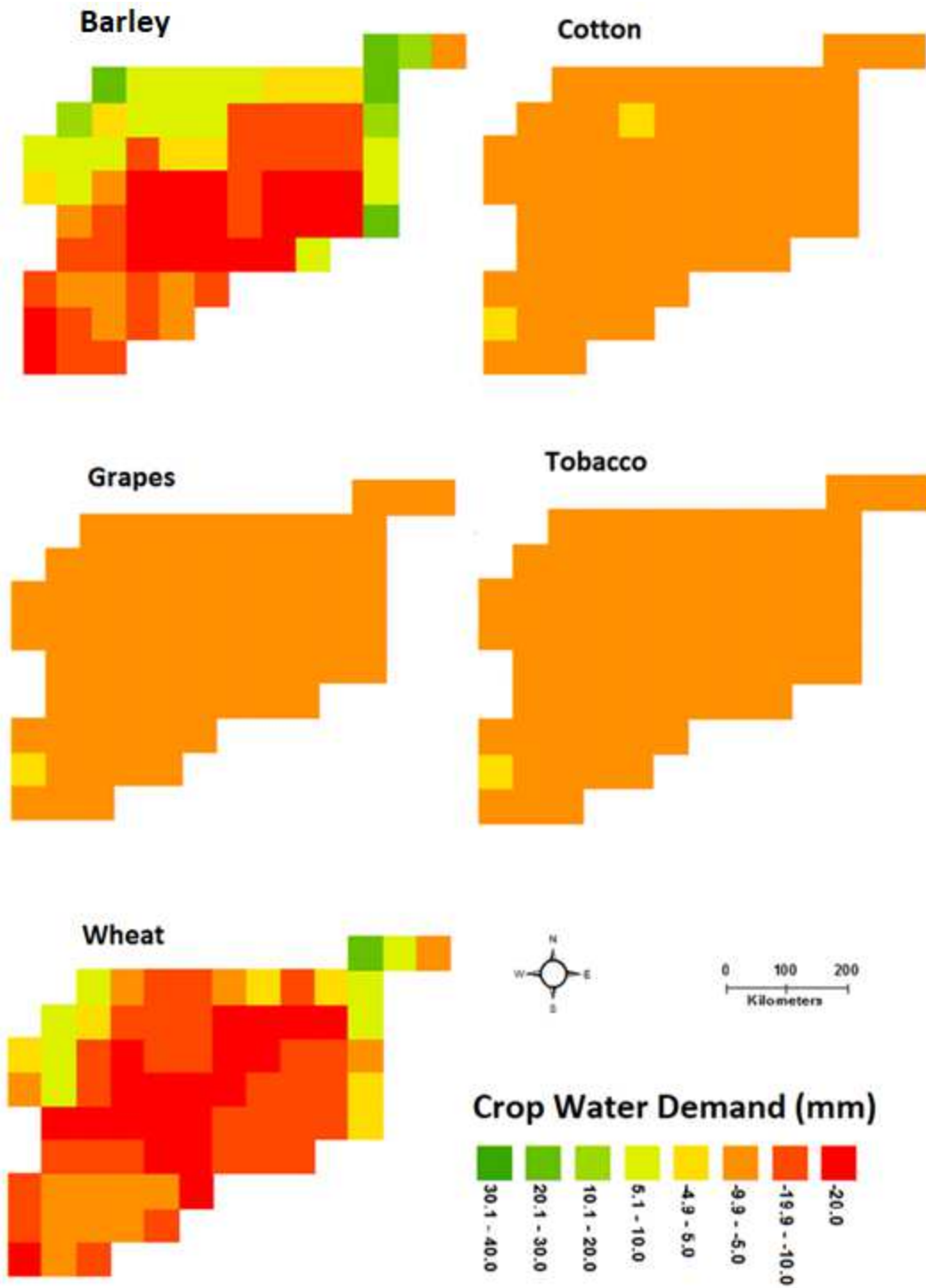


Figure 12 The difference in crops water availability in two periods (1951-1980) and (1981-2010)

5. Discussion

An increase in aridity during 1951-1980 compared to 1981-2010 has been discussed in previous studies (Houmsi et al., 2019). Around 6.21 percent of semi-arid land was detected to change to arid land during the two years, while 5.91 percent of dry sub humid land was observed to shift to semi-arid land. According to the findings, the main cause of Syria's rising aridity is a decrease in rainfall. About 28.3 percent of agricultural land in the north and northwest was discovered to be transitioning from tropical to dry-sub humid or dry-sub humid to semi-arid. The major cause of increasing aridity in Syria is believed to be a decline in rainfall, and it has the potential to alter crop water demand. The rising temperature is playing a major role in the changes in crop water demand. The aridity shift will have the greatest impact on forested and agricultural lands. Growing aridity may have a significant impact on land fertility and irrigation requirements. This may cause the increase in CWD which can affect the agriculture productivity and the agro-based industries due to the decrease in crop production leading to an economic instability in near future.

The CWD was found to increase mainly in the intensive agricultural area of Syria for the period 1951-2010. The increase was found more for winter crops compared to summer crops. The increase in CWD was found more in the southeast and the least in the northwest. The increase of aridity has been reported in many previous studies as the cause of a rise in irrigation requirements and therefore water stress. The present study validates this hypothesis also for Syria. However, the increase in CWD was found much higher in Syria which indicates a large effect of climate change on agriculture and water stress in the country. The increase in temperature was found to increase at majority of the location with hotter regions were getting hot as compared to the colder regions. The significant increase in temperature was observed in the northeast ($0.17^{\circ}\text{C}/\text{decade}$). The increase in Potential evapotranspiration was observed at most of the grid points following the same trend of increase in temperature. Changes in PET have caused significant increase in CWD for the period of 1981-2010 as compared to the base year 1951-1980. Except wheat crop, all the crops were found to suffer water scarcity compared to the early period.

Crop water availability in all the region of Syria was analyzed for the period of 1981-2010. The changes in the availability of crop water shows that for most of the crops the available water has been reduced up-to 20 mm/decade. The highest decrease is recoded for Barley with minimum changes for Tobacco and grapes. The reduction in water availability will cause the crop production and ultimately effecting the industries related to the agriculture.

Conclusion

This paper analyses the historical trends in CWD in addition to the changes in water availability for five different crops in Syria. The gridded data sets were used for the first time to analyze the changes in PET and CWD in the region. The Penman-Monteith method was used to measure the PET using gridded data, and the FAO-56 model was used to calculate crop water demand in this

article. . The study in this paper reported the increase in crop water demand in all the parts of Syria. Except for wheat, the largest increase in CWD was observed in April and May for all crops. The water availability for all five main crops was discovered to be decreasing in the area. With the maximum decrease for Barley and Wheat followed by the various decreasing rate of Tobacco, cotton and grapes. The change in climate caused the difference in rainfall and temperature, which is affecting the PET and CWD. The finding of the study is very useful in the agriculture development planning and irrigation designing purpose keeping in view the expected changes the region has face due to the variation in climate. Further studies can be performed following the framework developed in this study to calculate the potential changes in future CWD under various climate change scenarios and using different GCM simulations.

Declaration

The authors declare that this paper is the result of our own analysis and compilation. The paper his solely based on freely available data and all the authors have contributed in it.

Conflict of Interest

The authors declare that they have no known competing financial interests or personal relationships that could have appeared to influence the work reported in this paper.

Funding Statement

The author declares that no funding was received to complete this research from any organization

Author's Contribution

Conceptualization: [Rajab Homs], Methodology: [Shamsuddin Shahid], Formal analysis and investigation: [Shamsuddin Shahid], Writing - original draft preparation: [Zafar Iqbal]; Writing - review and editing: [Atif Muhammad Al, Ghaith FalahZiarh1]

Availability of data and material

The datasets generated during and/or analyzed during the current study are available from the corresponding author on reasonable request.

Code availability

The codes generated during the current study are available from the corresponding author on reasonable request.

Ethics approval

The author declares that all the ethical approvals were obtained prior to the submission of the manuscript from all the co-authors, whereas approvals from any funding agency is not applicable since no funds were received for this study.

Consent to participate

The author has the consent to participate in the review process of this manuscript as well as for the review of any others manuscript submitted to TAC for publication

Consent for publication

The authors show his full consent to approve this manuscript for publication in TAC.

Reference

- Acreman, M., Blake, J., Booker, D., Harding, R., Reynard, N., Mountford, J. & Stratford, C. 2009. A simple framework for evaluating regional wetland ecohydrological response to climate change with case studies from Great Britain. *Ecohydrology: Ecosystems, Land and Water Process Interactions, Ecohydrogeomorphology*, 2, 1-17.
- Ahmed, K., Iqbal, Z., Khan, N., Rasheed, B., Nawaz, N., Malik, I. & Noor, M. 2019. Quantitative assessment of precipitation changes under CMIP5 RCP scenarios over the northern sub-Himalayan region of Pakistan. *Environment, Development and Sustainability*, 1-15.
- Al-Furaiji, M., Karim, U. F., Augustijn, D. C., Waisi, B. & Hulscher, S. J. 2016. Evaluation of water demand and supply in the south of Iraq. *Journal of water reuse and desalination*, 6, 214-226.
- Asadi Zarch, M. A., Sivakumar, B., Malekinezhad, H. & Sharma, A. 2017. Future aridity under conditions of global climate change. *Journal of Hydrology*, 554, 451-469.
- Azad, N., Behmanesh, J., Rezaverdinejad, V. & Tayfeh Rezaie, H. 2018. Climate change impacts modeling on winter wheat yield under full and deficit irrigation in Myandoab-Iran. *Archives of Agronomy and Soil Science*, 64, 731-746.
- Bates, B., Kundzewicz, Z., Wu, S. & Palutikof, J. 2008. Climate Change and Water Technical Paper of the Intergovernmental Panel on Climate Change VI (IPCC, 2008). *There is no corresponding record for this reference.*[Google Scholar].
- Boretti, A. & Rosa, L. 2019. Reassessing the projections of the World Water Development Report. *npj Clean Water*, 2, 15.
- Brouziyne, Y., Abouabdillah, A., Hirich, A., Bouabid, R., Zaaboul, R. & Benaabidate, L. 2018. Modeling sustainable adaptation strategies toward a climate-smart agriculture in a Mediterranean watershed under projected climate change scenarios. *Agricultural Systems*, 162, 154-163.
- Buytaert, W. & De Bièvre, B. 2012. Water for cities: The impact of climate change and demographic growth in the tropical Andes. *Water Resources Research*, 48.
- El Kenawy, A. M. & McCabe, M. F. 2016. A multi-decadal assessment of the performance of gauge-and model-based rainfall products over Saudi Arabia: climatology, anomalies and trends. *International Journal of Climatology*, 36, 656-674.
- Houmsi, M. R., Shiru, M. S., Nashwan, M. S., Ahmed, K., Ziarh, G. F., Shahid, S., Chung, E.-S. & Kim, S. 2019. Spatial shift of aridity and its impact on land use of Syria. *Sustainability*, 11, 7047.
- Iqbal, Z., Shahid, S., Ahmed, K., Ismail, T. & Nawaz, N. 2019. Spatial distribution of the trends in precipitation and precipitation extremes in the sub-Himalayan region of Pakistan. *Theoretical and Applied Climatology*, 137, 2755-2769.
- Kar, G. & Verma, H. 2005. Climatic water balance, probable rainfall, rice crop water requirements and cold periods in AER 12.0 in India. *Agricultural Water Management*, 72, 15-32.
- Khan, N., Shahid, S., Ismail, T., Ahmed, K. & Nawaz, N. 2018. Trends in heat wave related indices in Pakistan. *Stochastic Environmental Research and Risk Assessment*.
- Lelieveld, J., Hadjinicolaou, P., Kostopoulou, E., Chenoweth, J., El Maayar, M., Giannakopoulos, C., Hannides, C., Lange, M. A., Tanarhte, M., Tyrlis, E. & Xoplaki, E. 2012. Climate change and impacts in the Eastern Mediterranean and the Middle East. *Climatic Change*, 114, 667-687.
- Liu, W., Fu, G., Liu, C. & Charles, S. P. 2013a. A comparison of three multi-site statistical downscaling models for daily rainfall in the North China Plain. *Theoretical and applied climatology*, 111, 585-600.
- Liu, Z.-F., Yao, Z.-J., Yu, C.-Q. & Zhong, Z.-M. 2013b. Assessing Crop Water Demand and Deficit for the Growth of Spring Highland Barley in Tibet, China. *Journal of Integrative Agriculture*, 12, 541-551.

- Mayowa, O. O., Pour, S. H., Shahid, S., Mohsenipour, M., Harun, S. B., Heryansyah, A. & Ismail, T. 2015. Trends in rainfall and rainfall-related extremes in the east coast of peninsular Malaysia. *Journal of Earth System Science*, 124, 1609-1622.
- Mehrotra, D. & Mehrotra, R. 1995. Climate change and hydrology with emphasis on the Indian subcontinent. *Hydrological sciences journal*, 40, 231-242.
- Miyan, M. A. 2015. Droughts in Asian least developed countries: Vulnerability and sustainability. *Weather and Climate Extremes*, 7, 8-23.
- Nam, W.-H., Hayes, M. J., Svoboda, M. D., Tadesse, T. & Wilhite, D. A. 2015. Drought hazard assessment in the context of climate change for South Korea. *Agricultural Water Management*, 160, 106-117.
- Nautiyal, S., Bhaskar, K. & Khan, Y. I. 2015. *Biodiversity of Semiarid Landscape*, Springer.
- Noor, M., Ismail, T., Shahid, S., Nashwan, M. S. & Ullah, S. 2019. Development of multi-model ensemble for projection of extreme rainfall events in Peninsular Malaysia. *Hydrology Research*, 50, 1772-1788.
- Sahour, H., Vazifedan, M. & Alshehri, F. 2020. Aridity trends in the Middle East and adjacent areas. *Theoretical and Applied Climatology*, 142, 1039-1054.
- Salman, S. A., Shahid, S., Ismail, T., Ahmed, K. & Wang, X.-J. 2018. Selection of climate models for projection of spatiotemporal changes in temperature of Iraq with uncertainties. *Atmospheric Research*, 213, 509-522.
- Samadi, S., Carbone, G., Mahdavi, M., Sharifi, F. & Bihamta, M. 2012. Statistical downscaling of climate data to estimate streamflow in a semi-arid catchment. *Hydrology & Earth System Sciences Discussions*, 9.
- Scherer, M. & Diffenbaugh, N. S. 2014. Transient twenty-first century changes in daily-scale temperature extremes in the United States. *Climate dynamics*, 42, 1383-1404.
- Sun, S., Li, C., Wu, P., Zhao, X. & Wang, Y. 2018. Evaluation of agricultural water demand under future climate change scenarios in the Loess Plateau of Northern Shaanxi, China. *Ecological Indicators*, 84, 811-819.
- Swain, D. L., Horton, D. E., Singh, D. & Diffenbaugh, N. S. 2016. Trends in atmospheric patterns conducive to seasonal precipitation and temperature extremes in California. *Science Advances*, 2, e1501344.
- Thorntwaite, C. W. 1948. An approach toward a rational classification of climate. *Geographical review*, 38, 55-94.
- Tsakiris, G. & Vangelis, H. 2005. Establishing a drought index incorporating evapotranspiration. *European water*, 9, 3-11.
- Wang, L. & Chen, W. 2014. A CMIP5 multimodel projection of future temperature, precipitation, and climatological drought in China. *International Journal of Climatology*, 34, 2059-2078.
- Wang, L., Ranasinghe, R., Maskey, S., Van Gelder, P. M. & Vrijling, J. 2016a. Comparison of empirical statistical methods for downscaling daily climate projections from CMIP5 GCMs: a case study of the Huai River Basin, China. *International journal of climatology*, 36, 145-164.
- Wang, X.-J., Zhang, J.-Y., Shahid, S., Guan, E.-H., Wu, Y.-X., Gao, J. & He, R.-M. 2016b. Adaptation to climate change impacts on water demand. *Mitigation and Adaptation Strategies for Global Change*, 21, 81-99.
- Wheeler, T., Daymond, A., Morison, J., Ellis, R. & Hadley, P. 2004. Acclimation of photosynthesis to elevated CO₂ in onion (*Allium cepa*) grown at a range of temperatures. *Annals of applied biology*, 144, 103-111.
- Zhang, Q., Li, J., Singh, V. P. & Bai, Y. 2012. SPI-based evaluation of drought events in Xinjiang, China. *Natural Hazards*, 64, 481-492.

Figures

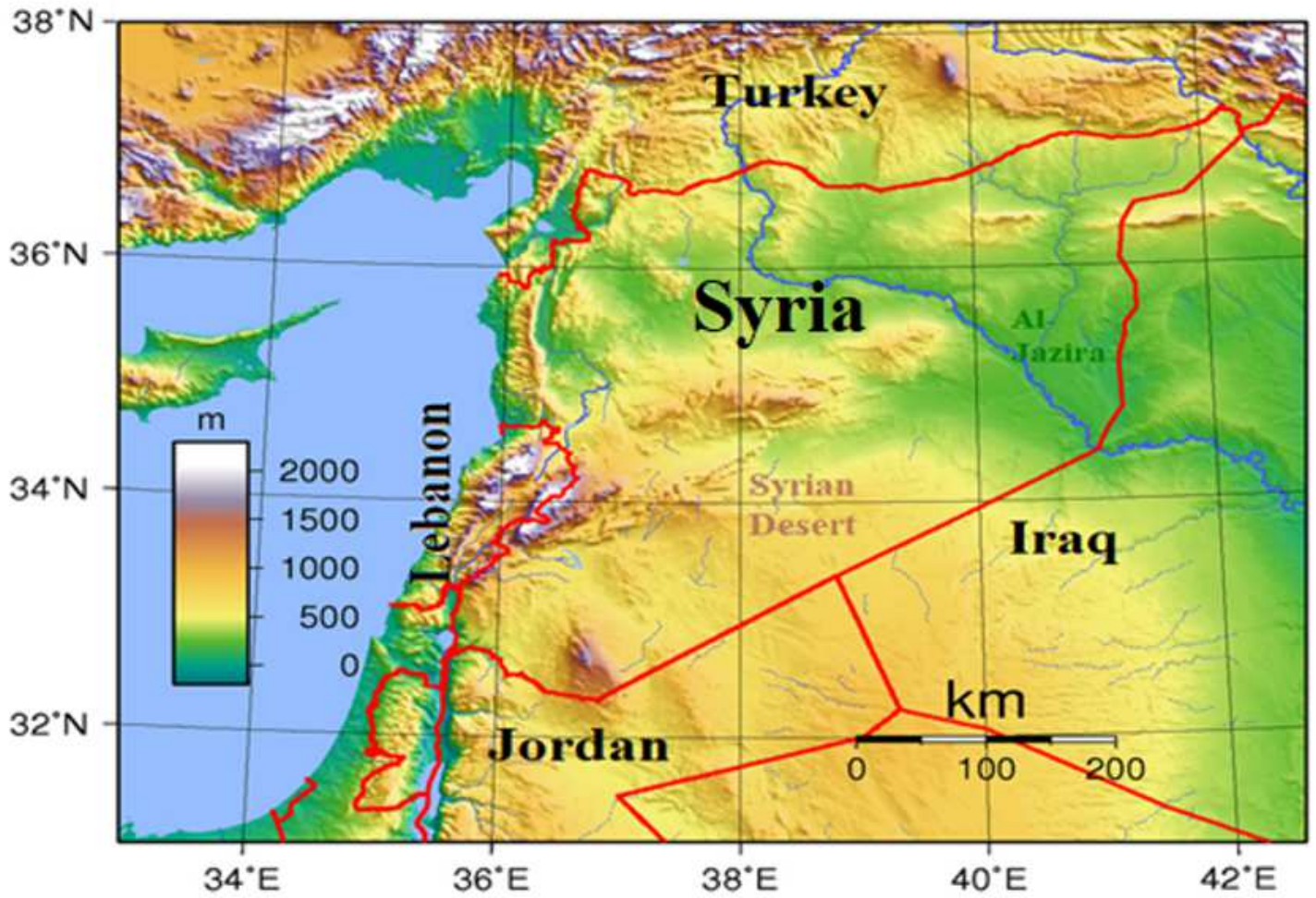


Figure 1

Location in the world and topography of Syria

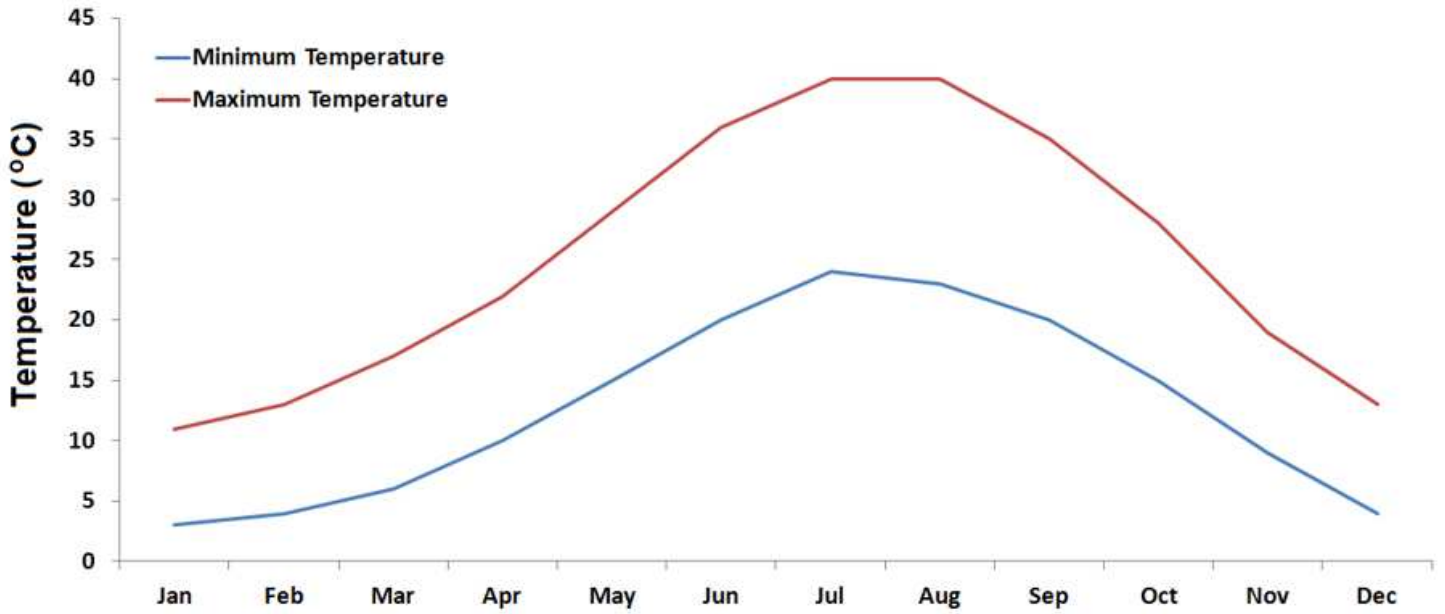


Figure 2

The seasonal variation of temperature of Syria estimated using climate research unit (CRU) temperature for the period 1951-2010.

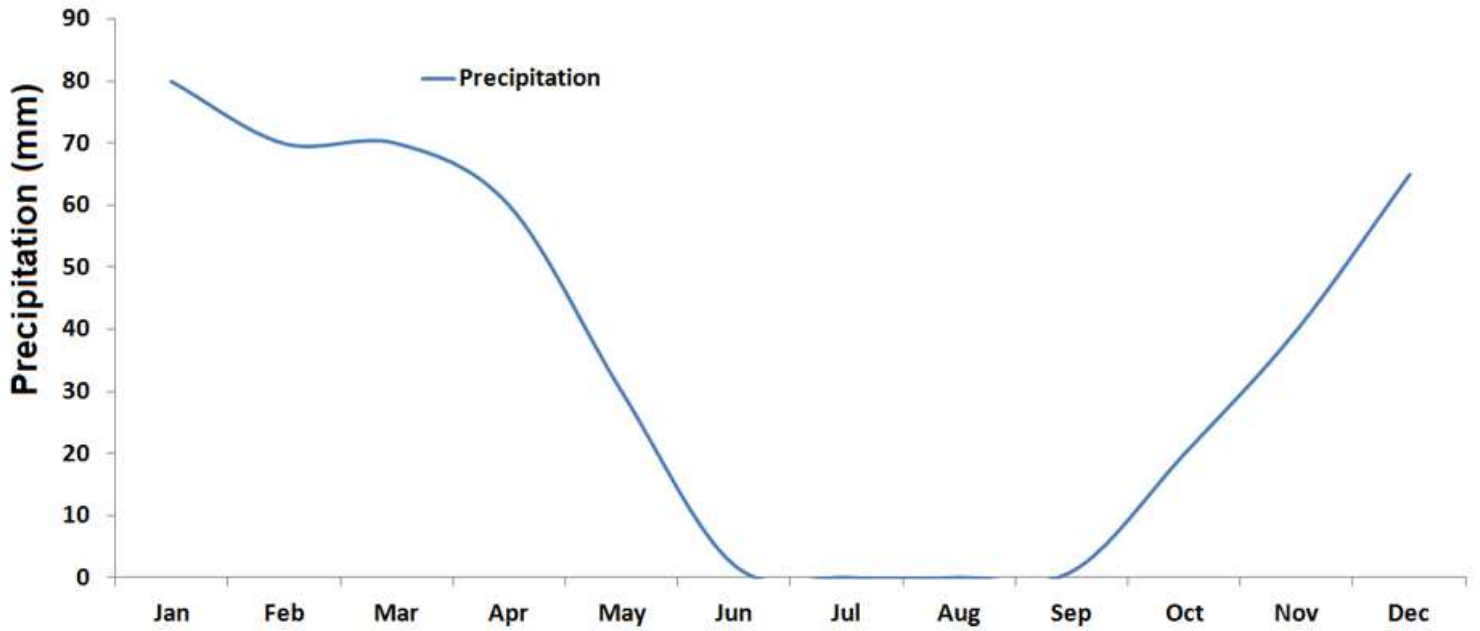


Figure 3

The seasonal variation of precipitation of Syria estimated using global precipitation climatology centre (GPCC) precipitation for the period 1951-2010

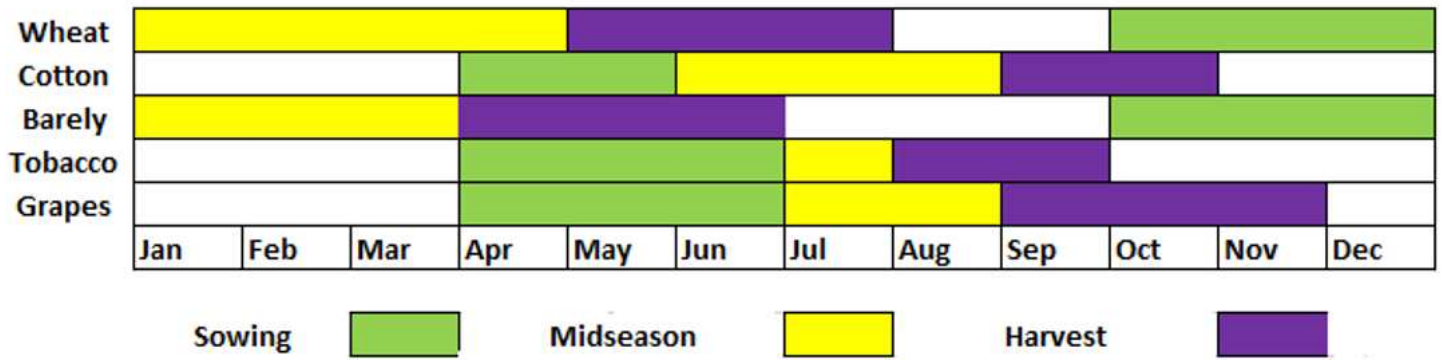


Figure 4

Calendar for selected main crops of Syria (FAO, 2017)

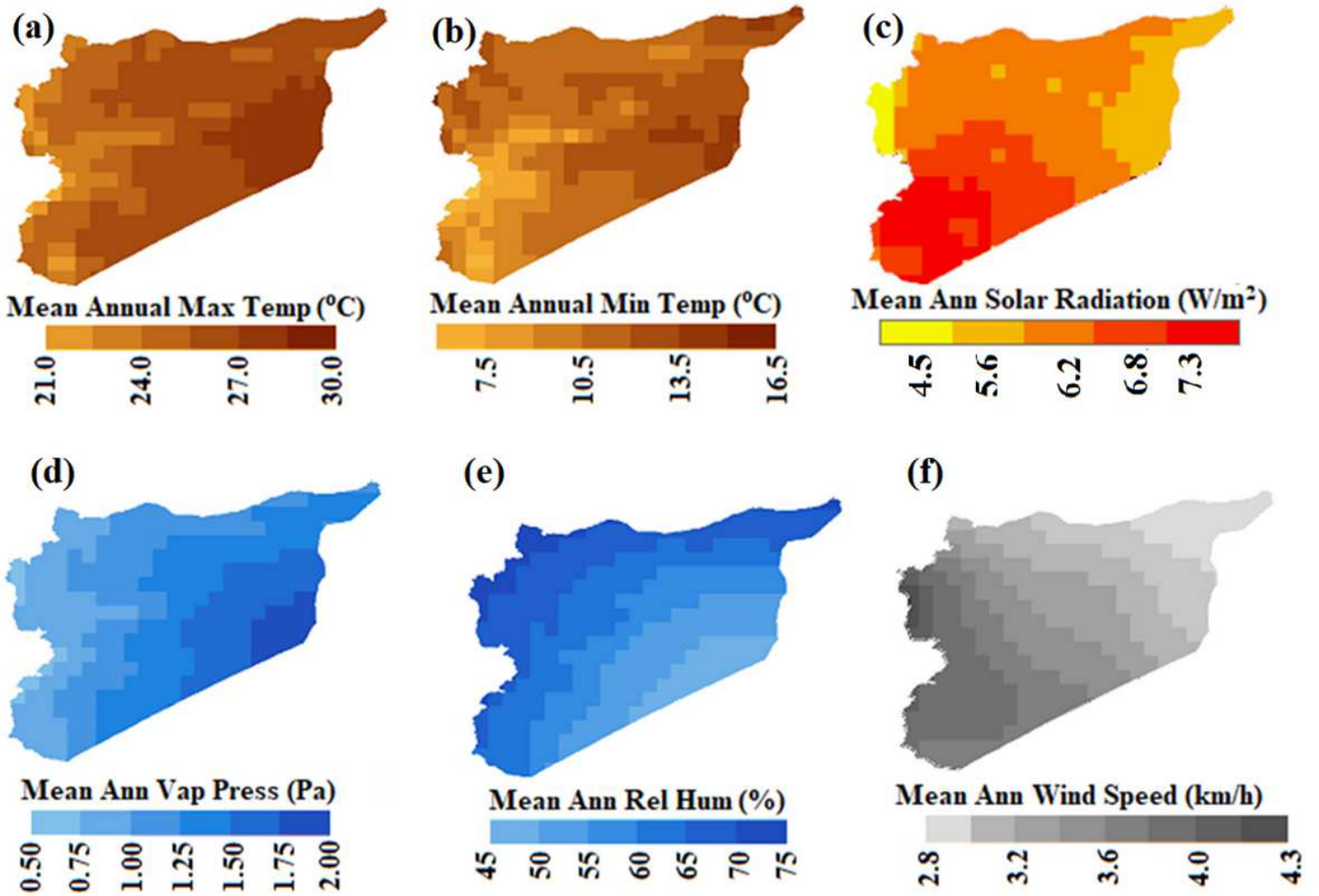
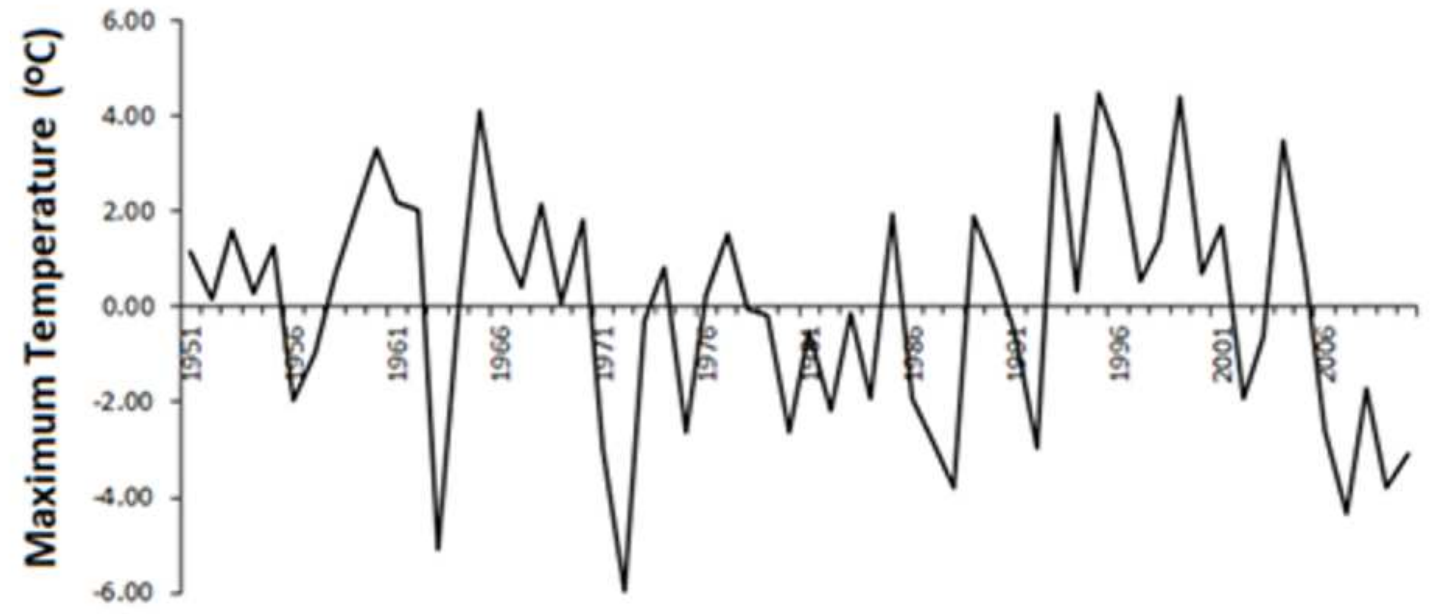
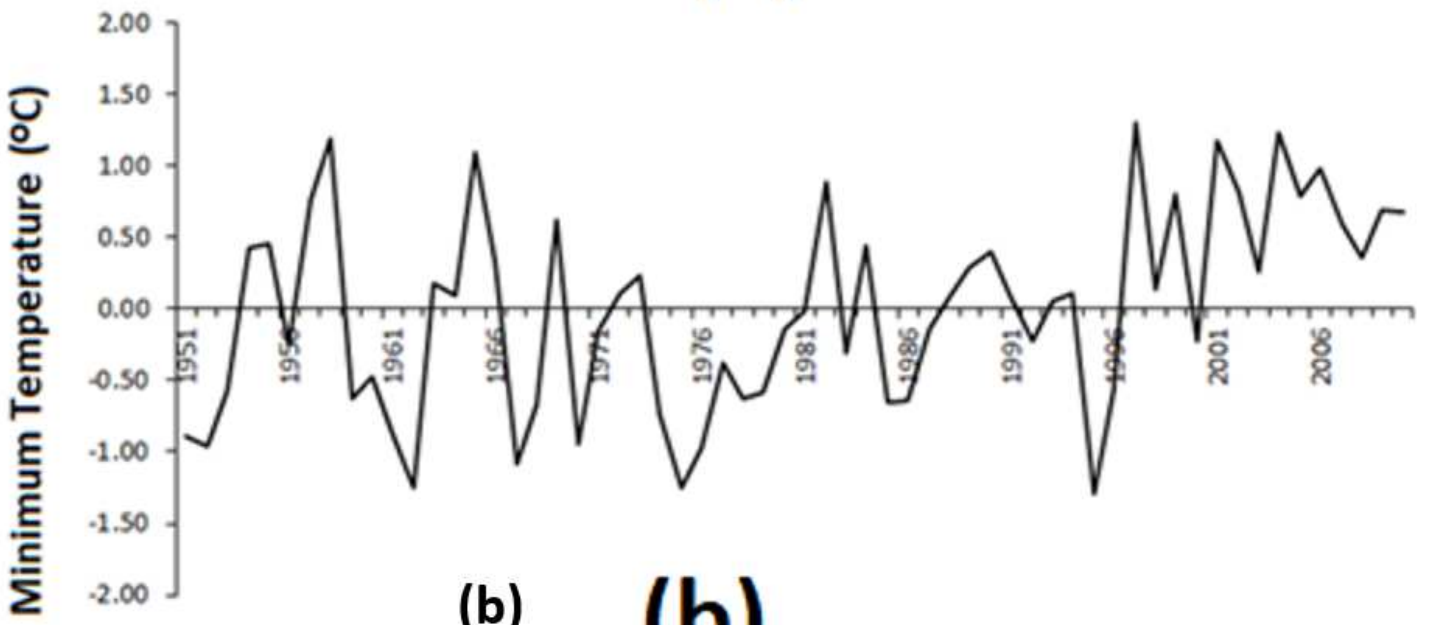


Figure 5

Annual Average of (a) Maximum Temperature (b) Minimum Temperature (c) Solar Radiation (d) Vapor Pressure (e) Relative Humidity (f) Wind Speed



(a) (a)



(b) (b)

Figure 6

Anomaly in an annual average of daily (a) maximum temperature, and (b) and minimum temperature

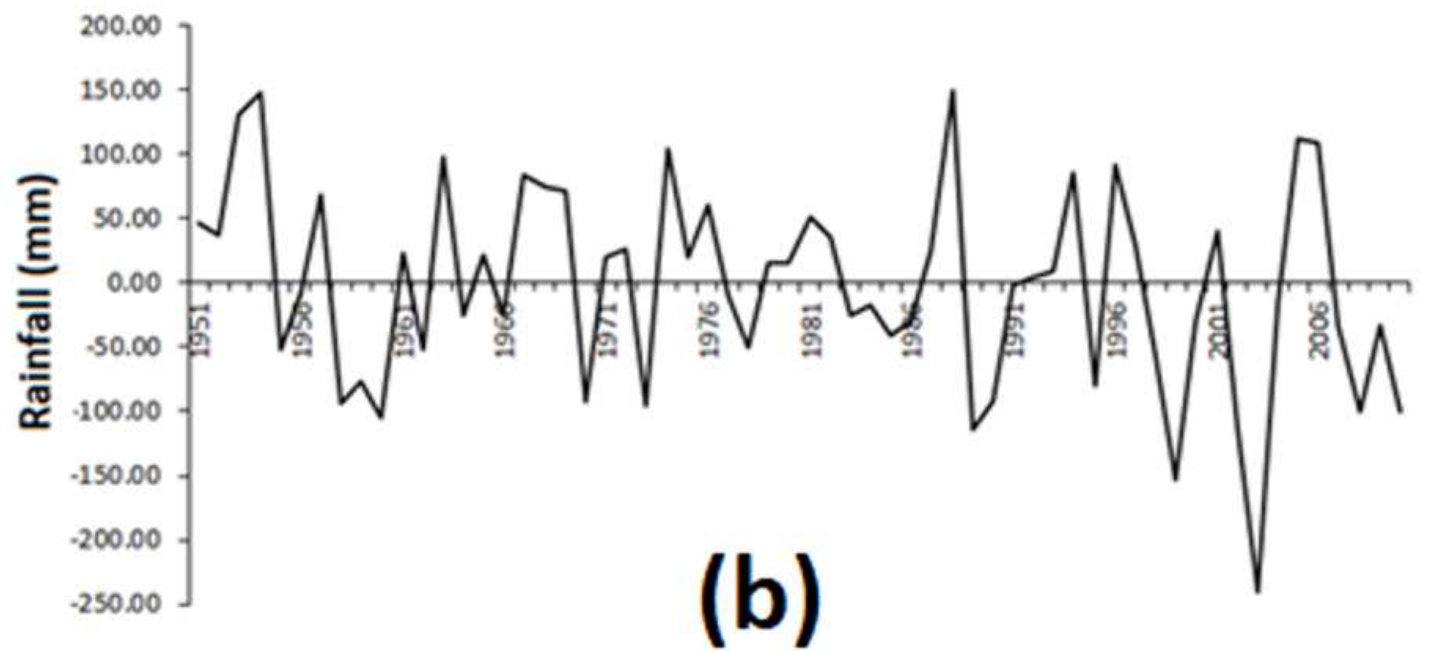
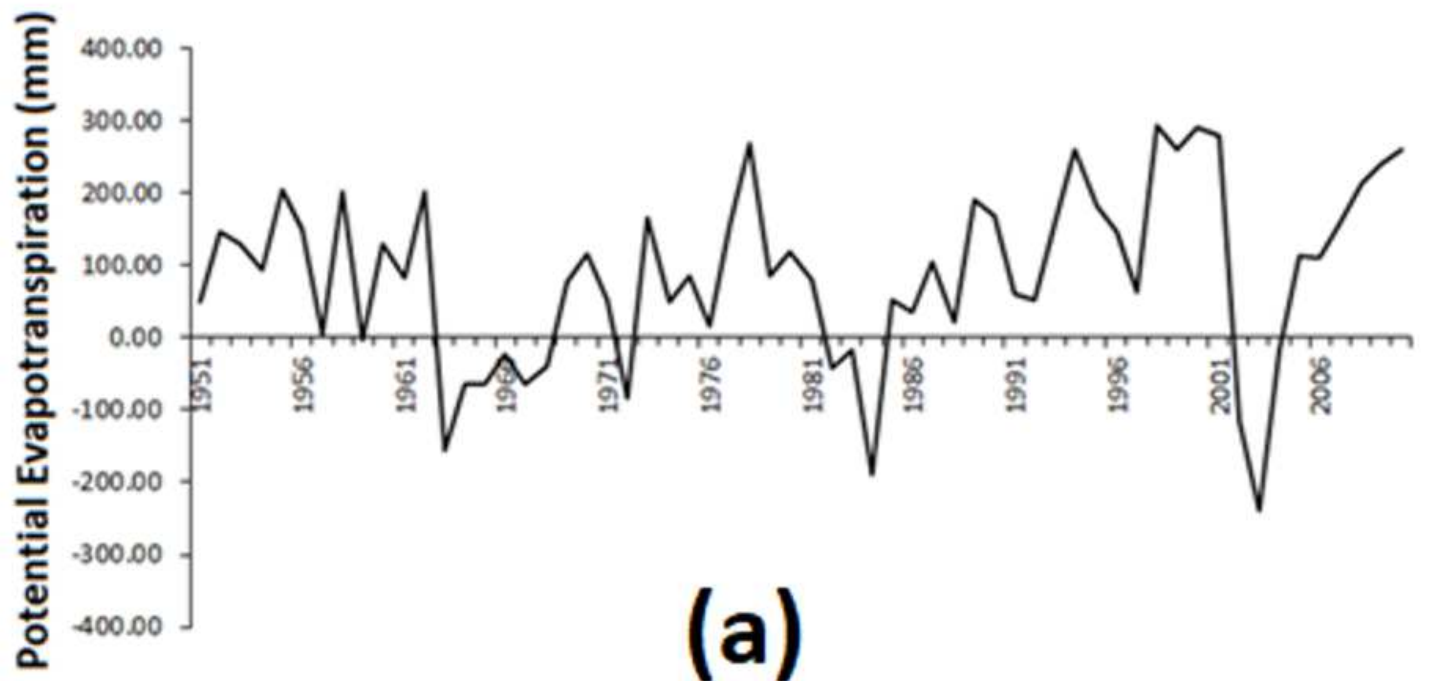
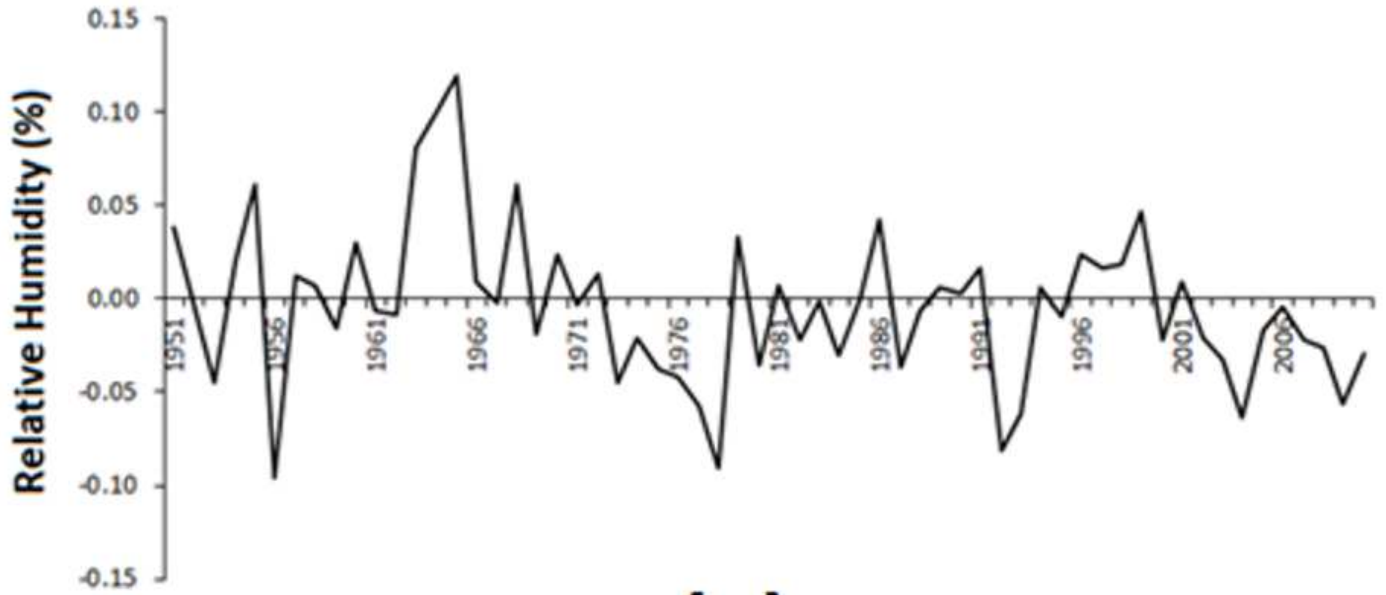
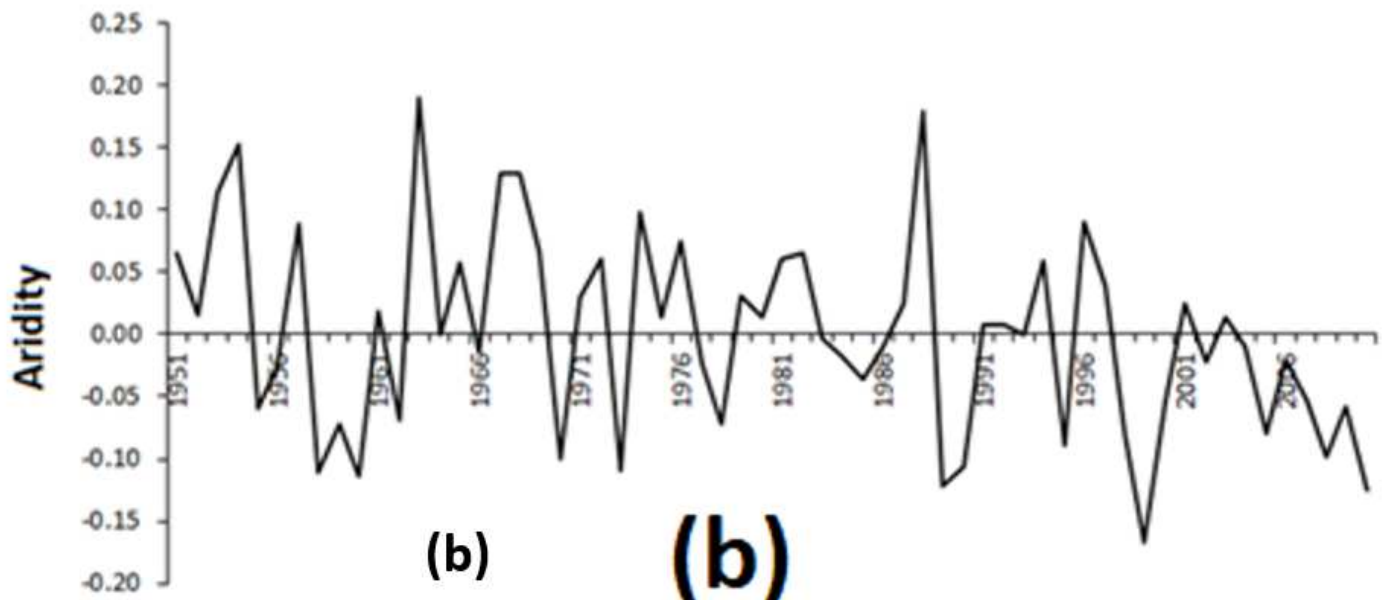


Figure 7

Anomaly in annual (a) potential evapotranspiration, and (b) rainfall



(a) (a)



(b) (b)

Figure 8

Anomaly in annual average (a) relative humidity, and (b) aridity

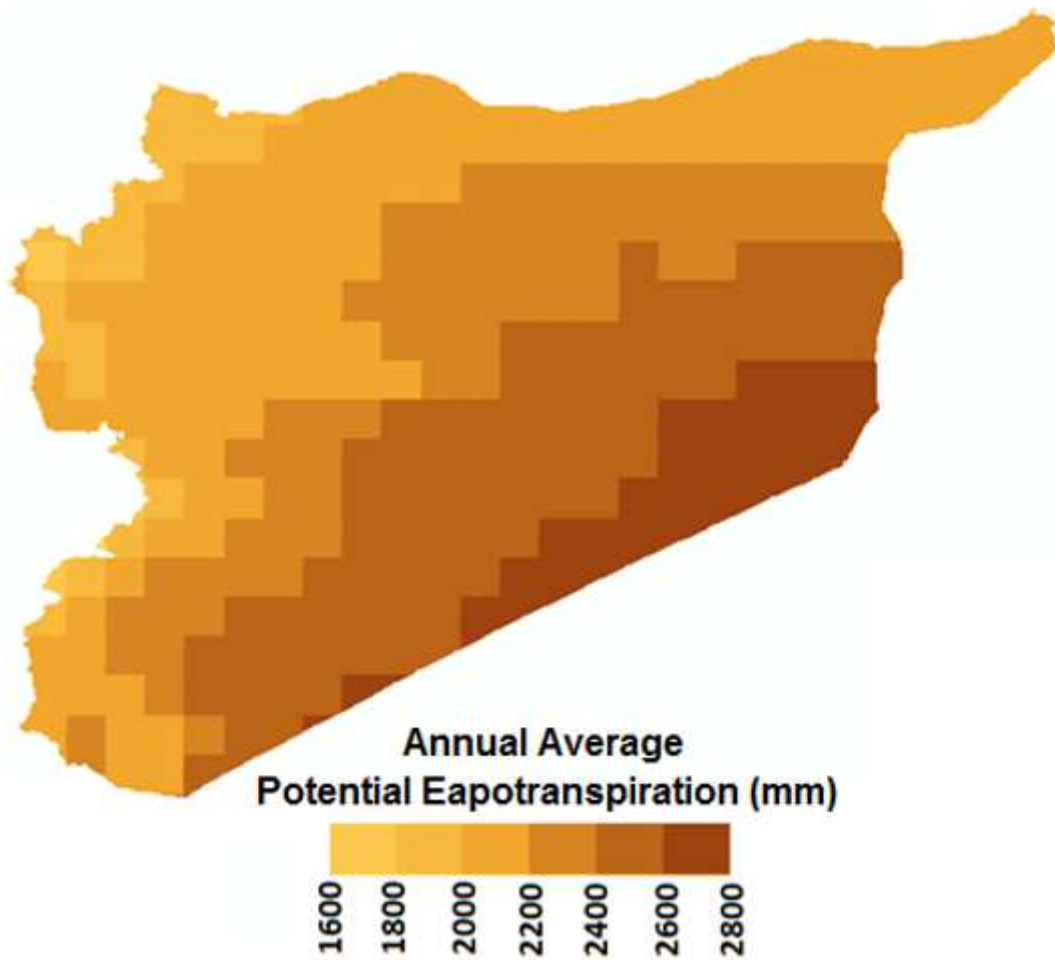


Figure 9

The Penman-Monteith method was used to calculate the spatial distribution of potential evapotranspiration (mm).

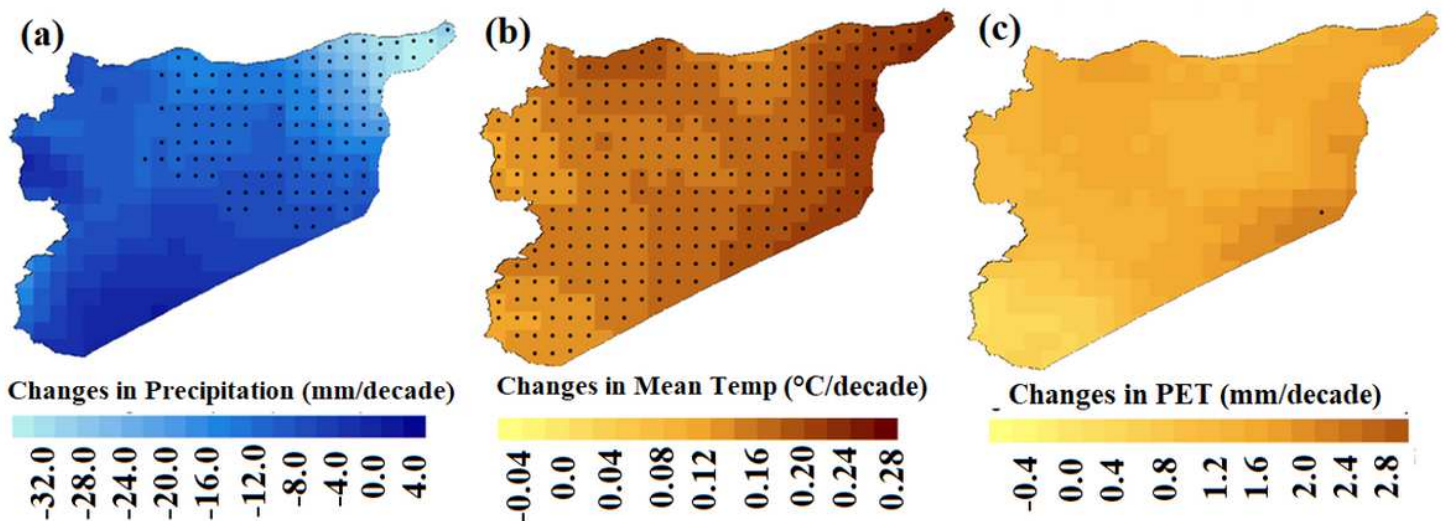


Figure 10

From 1951 to 2010, the spatial distribution of rainfall (a), temperature (b), and PET (c) . The Modified Mann Kendall trend test yielded significant trends at the 0.05 are marked as dots

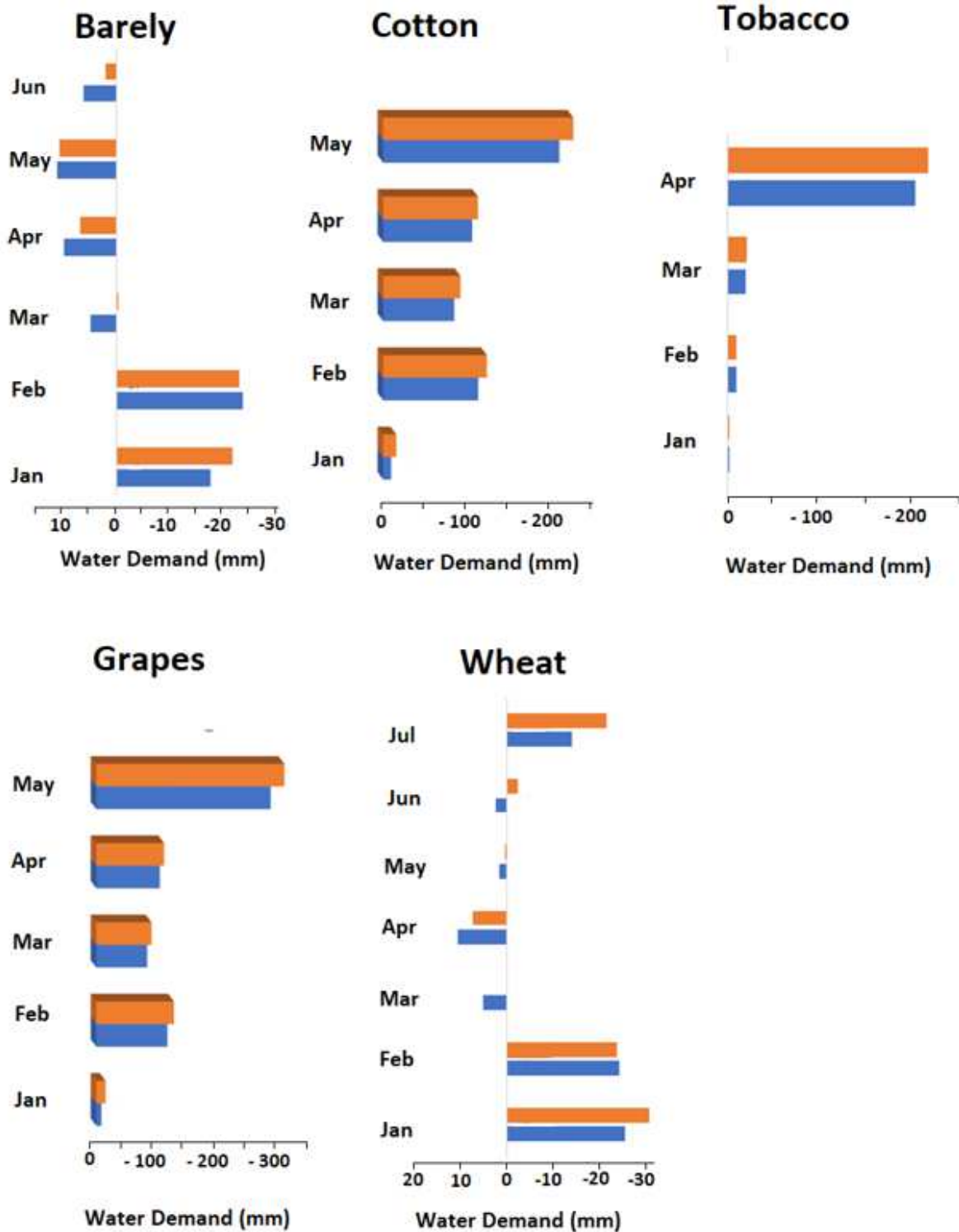


Figure 11

Changes in water demand of major crops of Iraq between 1951-1980 and 1981-2010

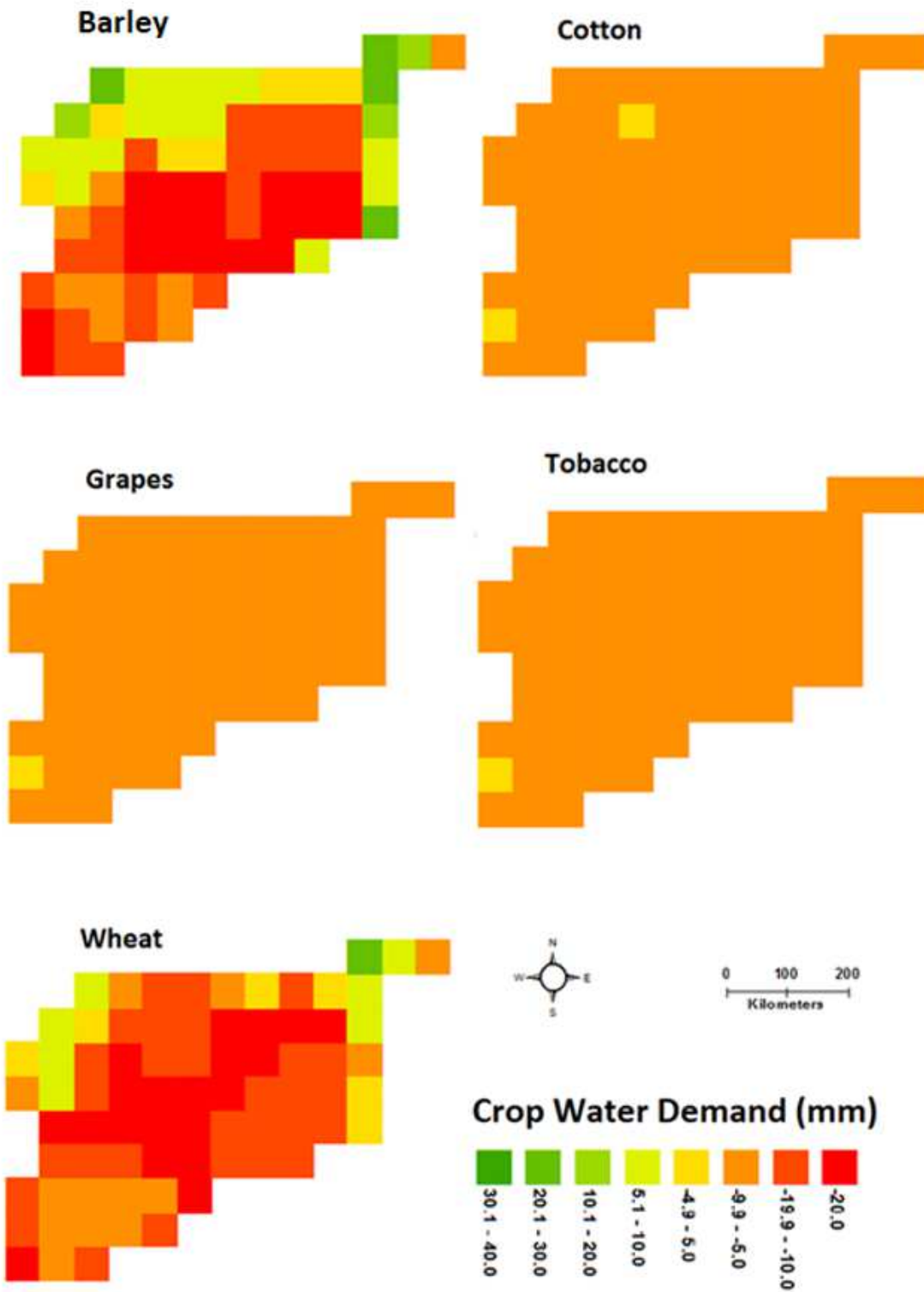


Figure 12

The difference in crops water availability in two periods (1951-1980) and (1981-2010)